Supplement of

The different sensitivities of aerosol optical properties to particle concentration, humidity, and hygroscopicity between the surface level and the upper boundary layer in Guangzhou, China

Xiaoai Jin[1], Zhanqing Li[2], Tong Wu[1], Yuying Wang[3], Yafang Cheng[4], Tianning Su[2], Jing Wei[1], Rongmin Ren[1], Hao Wu[5], Shangze Li[1], Dongmei Zhang[1], and Maureen Cribb[2]

[1]State Key Laboratory of Remote Sensing Science, College of Global Change and Earth System Science, Beijing Normal University, Beijing, 100875, China

[2]Department of Atmospheric and Oceanic Science and ESSIC, University of Maryland, College Park, Maryland, USA

[3]Key Laboratory for Aerosol-Cloud-Precipitation of China Meteorological Administration, School of Atmospheric Physics, Nanjing University of Information Science and Technology, Nanjing 210044, China

[4]Minerva Research Group, Max Planck Institute for Chemistry, 55128 Mainz, Germany

[5]College of Electronic Engineering, Chengdu University of Information Technology, Chengdu 610225, China
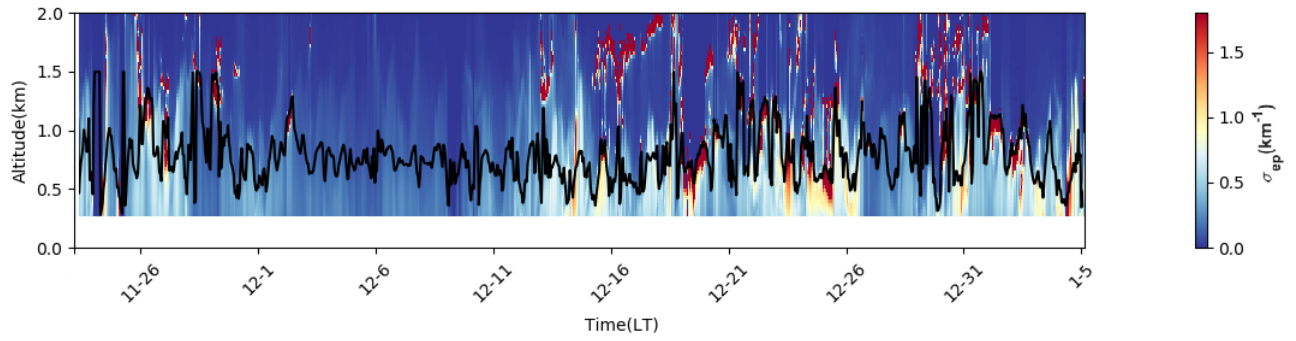
Correspondence to: Zhanqing Li (zhanqing@umd.edu)

Figure S1. Vertical profiles of aerosol extinction coefficient during the sampling period. The black line shows the planetary boundary layer height.
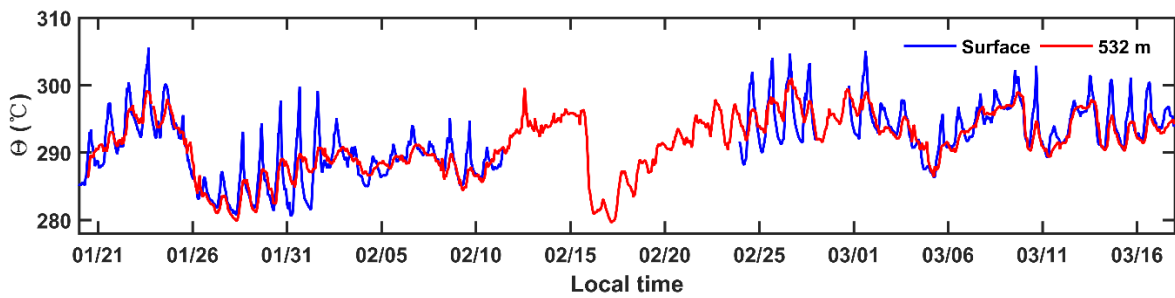

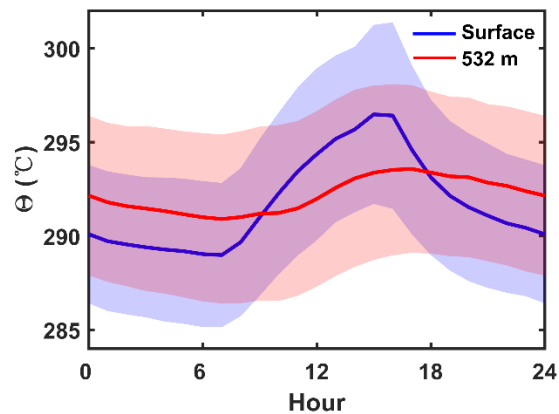**Figure S2. Time series of the potential temperature (θ) at the surface (blue line) and at 532 m (red line).**

Figure S3. Diurnal variations of potential temperature (θ) at the surface (blue line) and at 532 m (red line). Shaded areas represent standard deviations.

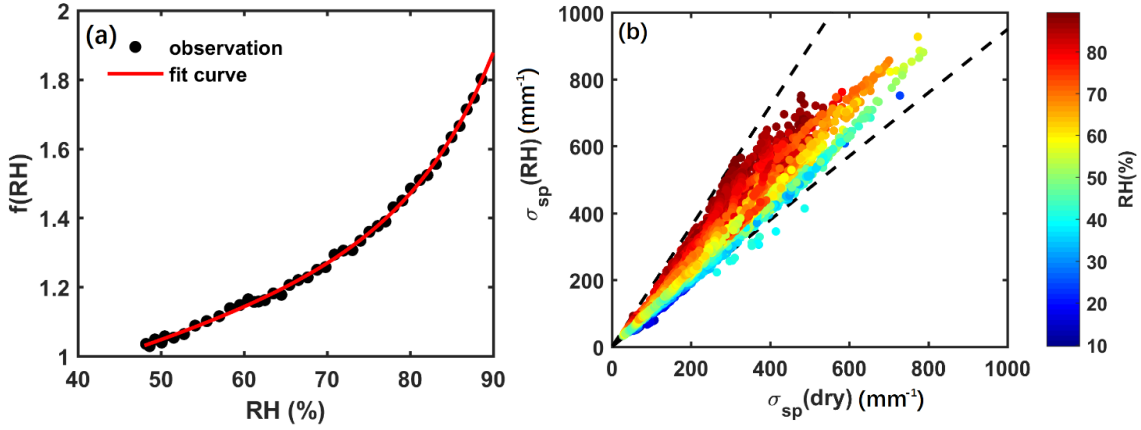**Figure S4. (a) One case showing the light scattering enhancement factor (f (RH)) as a function of RH. The red line is the best-fit curve through the data. (b) Comparison of the aerosol extinction coefficient in the dry state (σ$_{sp}$ (dry)) and under ambient RH conditions (σ$_{sp}$ (RH)). The color of the dots shows the ambient RH.**

Considering the uncertainties in the ISORROPIA II model, a comparison between the ALWC modeled by ISORROPIA II (ALWC$_{ISO}$) and the ALWC calculated based on measurements made by a humidified nephelometer system (ALWC$_{Hneph}$) was conducted, showing that these two results agree well (Fig. S3). ALWC$_{Hneph}$ was calculated using the humidified nephelometer system output based on the method proposed by Kuang et al. (2018). The proposed ALWC calculation method includes two main steps: (1) calculating the total volume in the dry state ($V_{a, dry}$) based on the particle number size distribution and (2) calculating the volume growth factor of the ambient aerosol particles ($V_{g, RH}$) due to water uptake using the light scattering enhancement factor and the Ångström exponent. The ALWC is then calculated as:

$$ALWC = V_{a,dry} \times (V_{g,RH} - 1).$$

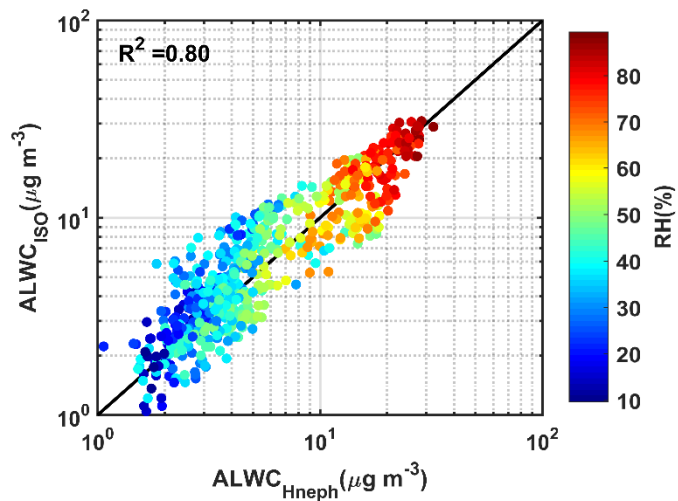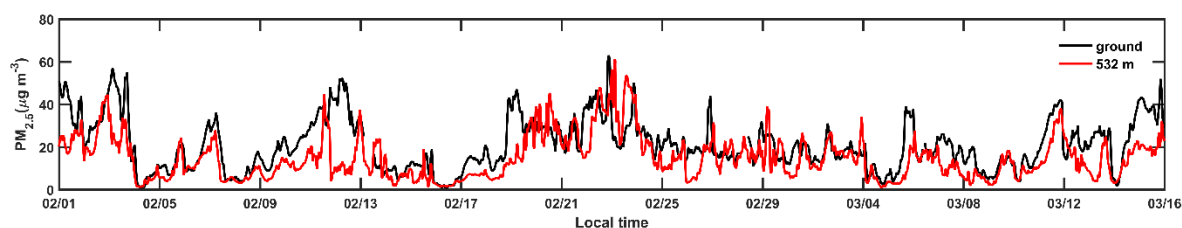**Figure S5. The aerosol liquid water content modeled by ISORROPIA-II (ALWC $_{ISO}$) as a function of measurements from a humidified nephelometer system (ALWC $_{Hneph}$). The color of the dots shows the ambient RH. ALWC $_{ISO}$ agree well with ALWC $_{Hneph}$.**

Figure S6. Time series of PM$_{2.5}$ mass concentrations at the surface (black line) and at 532 m (red line) from 1 February to 16 March 2020. PM$_{2.5}$ decreases both at the ground level and at 532 m due to the impact of the coronavirus (COVID-19) pandemic and subsequent lockdown during the second phase of the campaign.
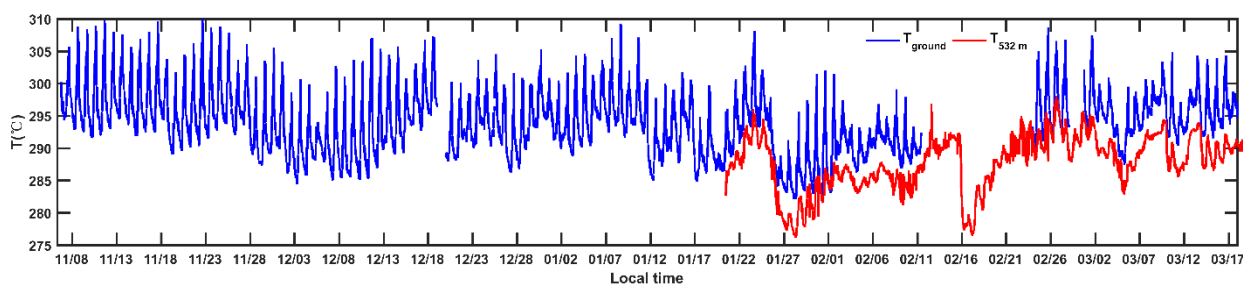
Figure S7. Time series of air temperature at the surface (blue line) and at the 532-m level of the Guangzhou tower (red line) during their respective observation periods.
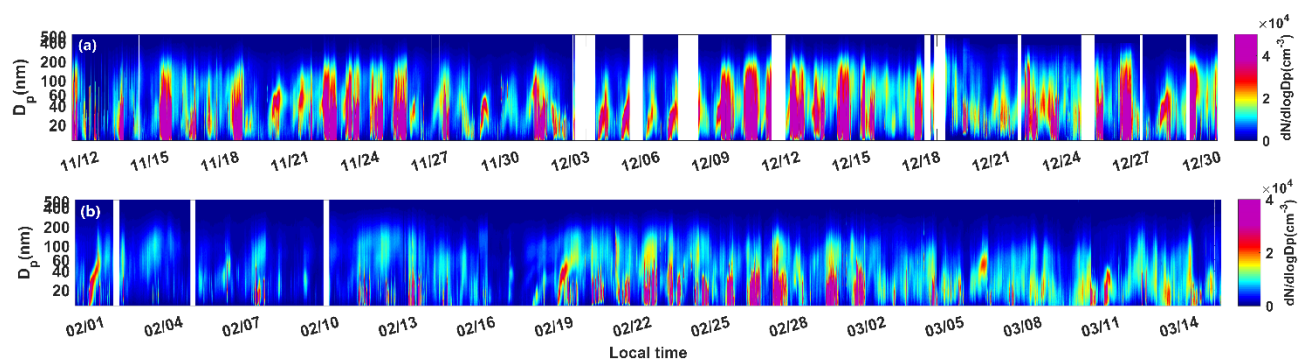
Figure S8. Time series of particle number size distributions at the surface during (a) the first and (b) second phases of the experiment.
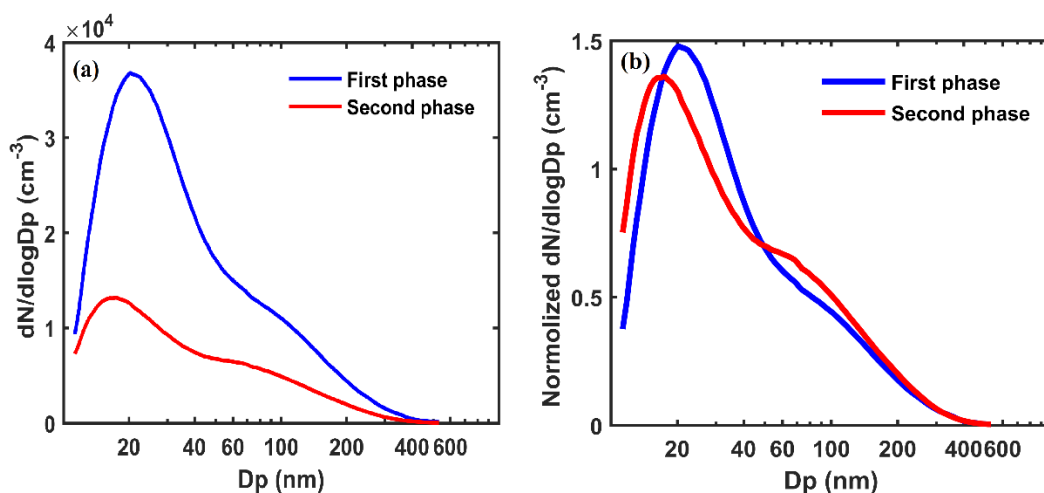
Figure S9. (a) Average PNSDs at the surface during the first phase (blue line) and second phase (red line) of the experiment; (b) normalized PNSDs at the surface during the first phase (blue line) and second phase (red line) of the experiment.
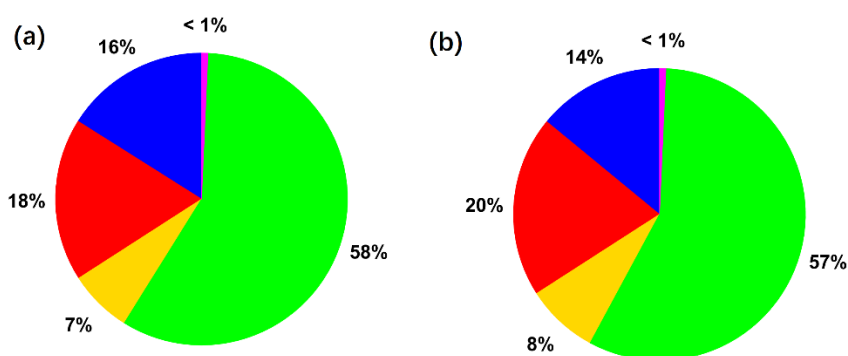

Figure S10. Mass fractions of different aerosol chemical species (a) at the surface and (b) at 532 m. Different colors represent different chemical species (see the legend in Fig. S11).
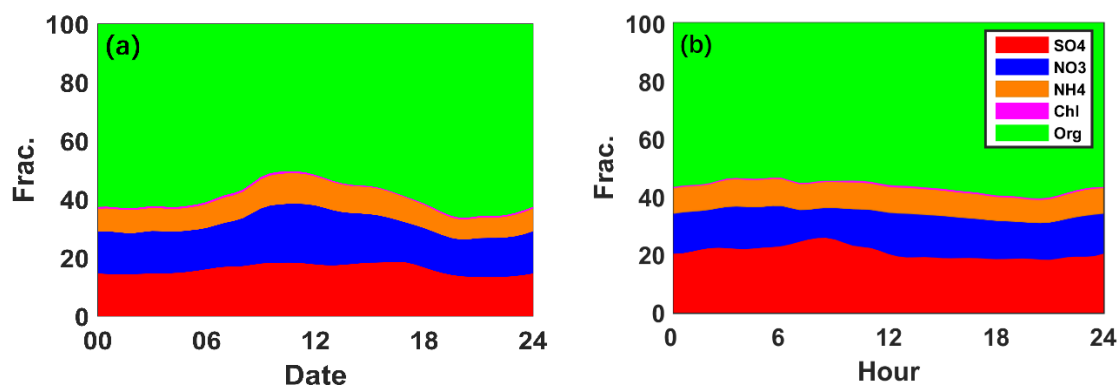

Figure S11. Diurnal variations of the mass fractions of different aerosol chemical species (a) at the surface and (b) at 532 m.
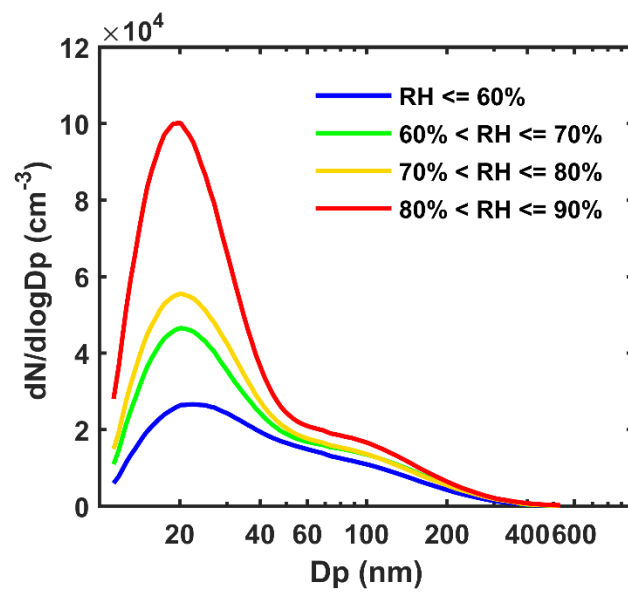
Figure S12. Average particle number size distributions at the surface for different RH ranges.